Internal Assessment: Chemistry

Investigating the relationship between the concentration of MnO_2 catalyst powder and the first order rate constant in the decomposition of H_2O_2 using measurements of pressure.

Research Question: How does changing the concentration of solid MnO_2 catalyst powder suspended in aqueous 1.1 % (v/v) H_2O_2 (aq) affect the first order rate constant for its decomposition at 24°C?

September 9, 2025

Word count: 1492

1 Introduction

Hydrogen peroxide is widely used in disinfection, bleaching, and environmental remediation. Its catalytic decomposition improves its oxidizing ability and is especially relevant in green chemistry due to the reduced waste generated. Transition metal ions such as manganese, iron, cobalt, and lead are commonly used to catalyze this reaction.[1] Manganese, in the form of MnO_2, is the catalyst of choice in this investigation because it is available in the school laboratory, being stable, inexpensive, and non-toxic in small quantities.

This investigation aims to establish a quantitative relation between the concentration of manganese oxide powder and the rate of decomposition of H_2O_2, by measuring the concentration of H_2O_2 indirectly through the amount of oxygen gas released. Theory states that for low amounts of MnO_2, the relationship between its mass and the observed first order rate constant.

2 Background Information

Most existing studies use MnO_2 catalysts immobilized on solid supports[2] or embedded in porous materials[4]. In contrast, this investigation uses fine MnO_2 powder suspended in solution. This setup presents practical limitations, most notably that the catalyst in its powdered form cannot be directly recovered after the reaction, necessitating an additional separation process. Nonetheless, the powdered form offers simplicity for a school laboratory.

Existing studies monitor the reaction utilizing methods such as titration on samples taken at specific intervals[1] or colorimetric methods[2], both of which allow direct measurement of the concentration of hydrogen peroxide in the solution. Instead, this ex-

periment opts to evaluate the progress of the reaction by measuring the amount of oxygen gas released by the reaction over time. This can be calculated with information about the pressure of the sealed reaction vessel over time, assuming constant temperature. Gas pressure will be measured using a pressure sensor, allowing for precise, continuous data collection suitable for computer processing.

2.1 Relevant Theory

> "The rate limiting reaction is believed to be the initial reaction between hydrogen peroxide and the iron oxides [5, 7, 6]. Additionally, the results reveal that the decomposition of H_2O_2 follows pseudo-first order kinetics:
>
> $$-\frac{\mathrm{d}[H_2O_2]}{\mathrm{d}t} = k_{\mathrm{app}}[H_2O_2] \tag{2.1}$$
>
> and thus:
>
> $$\ln\left(\frac{[H_2O_2]}{[H_2O_2]_0}\right) = -k_{\mathrm{app}}t \tag{2.2}$$
>
> where k_{app} is the apparent first order rate constant, and $[H_2O_2]$ and $[H_2O_2]_0$ are the concentrations of H_2O_2 in the solution at any time t and time zero, respectively.[3]"

The data presented in **Section 4** agrees with theory, that the reaction is pseudo-first order. The aim of this investigation is to measure how k_{app} changes in relation to the amount of catalyst used.

Now a general expression for pressure as a function of time will be mathematically derived from (2.2).

Notation			
$n(\mathrm{H_2O_2})$	$\mathrm{H_2O_2}$ in solution at time t	P	Pressure at time t
$n(\mathrm{O_2})$	$\mathrm{O_2}$ released up to t	P_0	Initial pressure
n_0	Initial $\mathrm{H_2O_2}$ in solution	P_∞	Final pressure
n_{air}	Initial air molecules	V_l	Solution volume
R	Ideal gas constant	V_f	Flask volume
T	Temperature	V_g	$= V_f - V_l$, Gas volume

The catalysed decomposition is

$$2\,\mathrm{H_2O_2\,(aq)} \xrightarrow{\mathrm{MnO_2}} 2\,\mathrm{H_2O\,(l)} + \mathrm{O_2\,(g)}$$

From stoichiometry,

$$n(\mathrm{O_2}) = \frac{n_0 - n(\mathrm{H_2O_2})}{2} \quad \Longrightarrow \quad n(\mathrm{H_2O_2}) = n_0 - 2\,n(\mathrm{O_2}).$$

With $[\mathrm{H_2O_2}] = n(\mathrm{H_2O_2})/V_l$ and $PV_g = (n_{\mathrm{air}} + n(\mathrm{O_2}))RT$,

$$n(\mathrm{O_2}) = \frac{PV_g}{RT} - n_{\mathrm{air}}$$

so

$$[\mathrm{H_2O_2}] = \frac{n_0 + 2n_{\mathrm{air}} - 2PV_g/(RT)}{V_l}$$

At completion $n(\mathrm{H_2O_2}) = 0$, hence $n_0 + 2n_{\mathrm{air}} = 2P_\infty V_g/(RT)$ and therefore

$$[\mathrm{H_2O_2}] = \frac{2(P_\infty - P)\,V_g}{RT\,V_l}$$

Combining this with the integrated pseudo–first order law

$$-k_{\mathrm{app}}t = \ln\frac{[\mathrm{H_2O_2}]}{[\mathrm{H_2O_2}]_0}, \qquad [\mathrm{H_2O_2}]_0 = \frac{n_0}{V_l}$$

and simplifying yields

$$2(P_\infty - P)\frac{V_g}{RT} = n_0 e^{-k_{\text{app}}t}$$

and hence

$$P(t) = P_\infty - \frac{n_0 RT}{2V_g}\, e^{-k_{\text{app}}t}$$

For brevity define

$$c := \frac{n_0 RT}{2V_g},$$

giving the general form

$$\boxed{P(t) = P_\infty - c\, e^{-k_{\text{app}}t}}.$$

2.2 Existing Results

For pyrolusite (the primary manganese ore) powder, the highest reported specific rate constant is

$$k_{\text{pyro}} = 0.061\,\text{min}^{-1}\,\text{mM}^{-1},$$

measured at room temperature in 200 mL of solution containing 29.4 mM H_2O_2.[2] This suggests that the rate constant is proportional to the concentration of MnO_2 in solution.

The results obtained in this investigation will be compared with this result. **Hypothesis.** Ideally a proportional relationship between the mass of MnO_2 and k_{app} is observed in this investigation, and the result does not deviate majorly from the above value.

3 Experimental

3.1 Materials & Apparatus

Materials	
33% (v/v) H_2O_2 (aq), diluted to 3.3%	10 ± 0.5 mL per trial
Pure distilled water	20 ± 0.5 mL per trial
Fine MnO_2 powder	$\approx$ 1g total
Equipment	
220 mL Erlenmeyer flask	Thermometer
20 mL Medical syringe ($\pm$0.5 mL)	Electronic scale ($\pm$0.001 g)
Vernier Pressure sensor[1]	Rubber stopper
Magnetic stir bar and stir plate	Parafilm

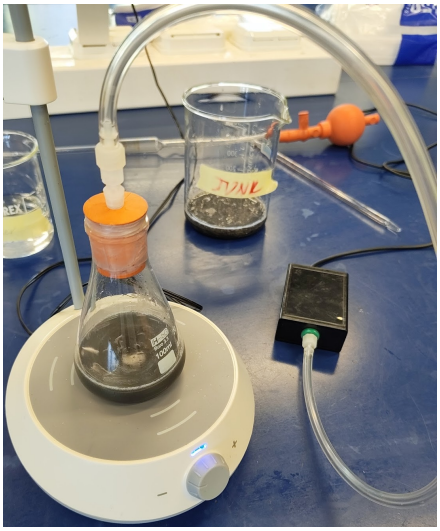

Figure 1: Apparatus

Pressure sensor specifications.

Range: 0–140 kPa Accuracy: $\pm$2 kPa Sampling rate: 1 Hz

Data is recorded automatically using Logger Pro.

Illustration. The stir bar is in the flask, which is sealed airtight with a rubber stopper wrapped in parafilm. The tapered valve connector of the pressure sensor is wrapped in parafilm and inserted in the hole of the rubber stopper. A minimal setup, with the aid of parafilm and pressure-rated tubing aims to minimize leakage at moderate ($\leq$ 140 kPa) pressure.

3.2 Process

Preparation: A 3.3% (v/v) H_2O_2 solution was prepared in advance. The pressure sensor was connected to the valve connector with tubing and verified to be functional.

Each trial: An empty Erlenmeyer flask was charged with 20 mL of water and the desired mass of MnO_2. The solution temperature was confirmed at 24°C. A stir bar was added, and stirring was maintained at 600 rpm. The rubber stopper was wrapped with parafilm and fitted securely to minimize leakage. Separately, 10 mL of 3.3% H_2O_2 was drawn into a syringe. The tapered region of the valve connector was wrapped with parafilm before the syringe contents were injected into the flask through the stopper, after which the connector was immediately inserted. The reaction was allowed to proceed until the pressure reached 140 kPa, at which point the connector was withdrawn. The solution temperature was checked again to ensure it remained near its initial value. The apparatus was then reset for subsequent trials.

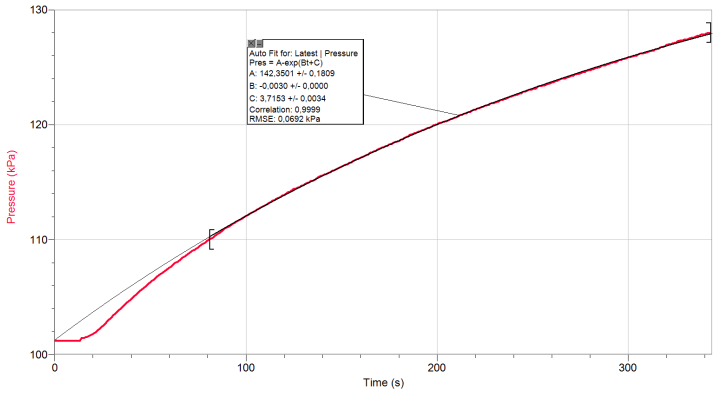

Figure 2: 0.05 g Trial Plot and Auto Fit

3.3 Analytical Method

With data on the relation between pressure and time, simply use Logger Pro's 'fit curve' functionality to automatically fit a curve with the general form derived in (2.11).

The curve will be fit on the data between 120 kPa and 140 kPa, except for the m(MnO_2)=0.05g. The beginning of data collection is avoided because it contains an unwanted artifact resulting from connecting the valve. Using the Auto Fit functionality also automatically gives the error radius for k_{app}, which is the only error among dependent variables that needs to be considered. To establish proportionality with respect to catalyst concentration, the error radius of MnO_2 mass and solution volume are also necessary.

In **Figure 2**, $A = P_\infty$, $B = -k_{\text{app}}$, and $C = \ln(c)$, in relation to the constants in (2.11). From this data, only the value of k_{app} is ultimately needed, but P_∞ is a useful sanity check, to ensure no major systematic error is taking place.

4 Results and Discussion

4.1 Computing Theoretical Final Pressure

We compute the theoretical final pressure and compare it to the experimental values given by Logger Pro, to avoid major errors.

$$\rho(H_2O_2) = 1.45 \text{ g mL}^{-1}, \qquad M(H_2O_2) = 34.0 \text{ g mol}^{-1},$$

$$\begin{aligned} V_l &= 30 \pm 1 \text{ mL} \\ \implies V_{H_2O_2} &= 0.33 \pm 0.011 \text{ mL} \\ \implies m &= \rho V = 0.33 \cdot 1.45 = 0.4785 \pm 0.0160 \text{ g}, \end{aligned}$$

$$n(H_2O_2) = \frac{m}{M} = \frac{0.4785}{34.0} = 0.0141 \pm 0.00047 \text{ mol} \tag{4.1}$$

This decomposes into 0.00705 ± 0.00024 mol O_2. Assuming constant gas volume

and temperature, the ideal gas law states

$$\Delta P = (\Delta n)\ R\ T\ V^{-1} \qquad \text{for } R \approx 8.314L \text{ kPa } K^{-1} \text{ mol}^{-1} \tag{4.2}$$

Initial conditions for the headspace gas:

$P_i = 101 \pm 1$ kPa, $V_g = 200 \pm 10$ mL $= 0.20 \pm 0.01$ L, $T = 24 \pm 1^\circ$C $= 297.15 \pm 1$ K

Then numerically $\Delta P = \dfrac{0.00705 \cdot 8.314 \cdot 297.15}{0.20} \approx 88 \pm 7$ kPa. The final pressure P_∞, in theory, is $P_0 + \Delta P \approx 88 + 102 = 190 \pm 8$ kPa. This is a rough range close to which the experimental final pressure should belong.

4.2 Data and Processing

$m(MnO_2)$	k_{app}	P_∞
0.05 g	$0.003043 \pm 0.000025\ s^{-1}$	142.35 ± 0.18 kPa
0.10 g	$0.003454 \pm 0.000023\ s^{-1}$	167.30 ± 0.24 kPa
0.15 g	$0.005248 \pm 0.000055\ s^{-1}$	176.15 ± 0.48 kPa
0.20 g	$0.006974 \pm 0.000106\ s^{-1}$	176.66 ± 0.70 kPa
0.10 g	$0.005308 \pm 0.000053\ s^{-1}$	176.98 ± 0.46 kPa

Table 1: Trial Data From Logger Pro

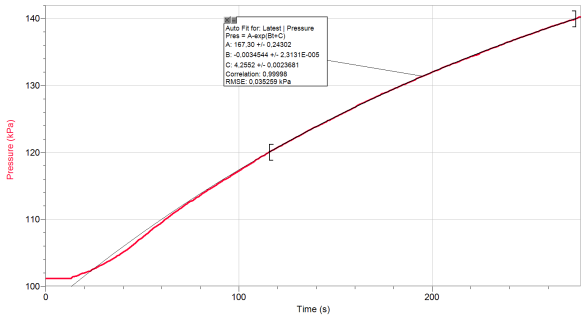

Figure 3: $m(MnO_2) = 0.10$ g

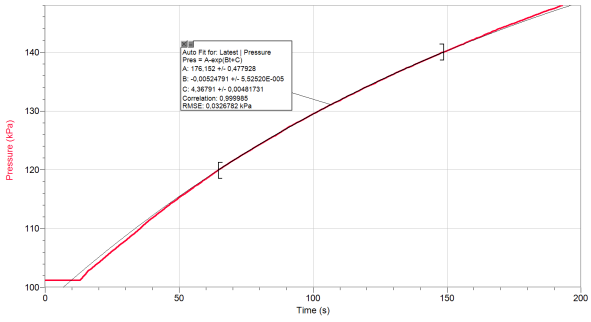

Figure 4: $m(MnO_2) = 0.15$ g

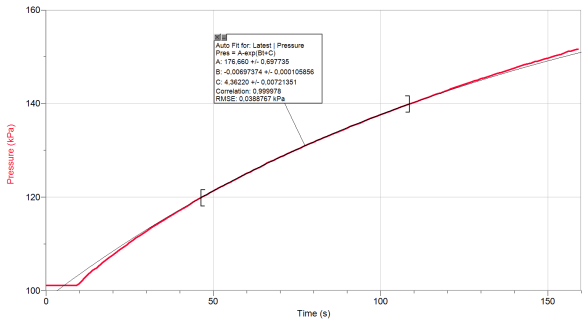

Figure 5: $\mathrm{m(MnO_2)} = 0.20$ g

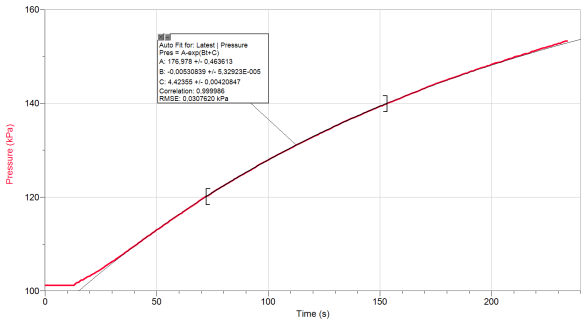

Figure 6: $\mathrm{m(MnO_2)} = 0.25$ g

It seems that P_∞ in practice is always below the theoretical P_∞ derived in **Section 4.1**. The deviation is not major, and is likely caused by the reasons discussed in **Section 5**.

For each trial, we compute the concentration of $\mathrm{MnO_2}$:

$$c(\mathrm{MnO_2}) = \frac{n(\mathrm{MnO_2})}{V_l} = \frac{m(\mathrm{MnO_2})}{M(\mathrm{MnO_2})V_l} = 383.4 \text{ mM } g^{-1} \cdot m(\mathrm{MnO_2})$$

The uncertainty of this is 3.3% resulting from $V_l = 30 \pm 1$ mL; the uncertainty of catalyst mass is negligible.

$\mathrm{m(MnO_2)}$	$\mathrm{c(MnO_2)}$
0.05 g	19.17 ± 0.63 mM L^{-1}
0.10 g	38.34 ± 1.27 mM L^{-1}
0.15 g	57.51 ± 1.90 mM L^{-1}
0.20 g	76.68 ± 2.53 mM L^{-1}
0.10 g	95.85 ± 3.16 mM L^{-1}

Table 2: Catalyst Concentrations

The aim is to find a proportional relationship in between the concentrations in **Table 2** and the corresponding rate constants in **Table 1**. Plotting the data points of the form $(c(\mathrm{MnO_2}), k_{\text{app}})$, each representing a different trial, **Figure 7** is obtained.

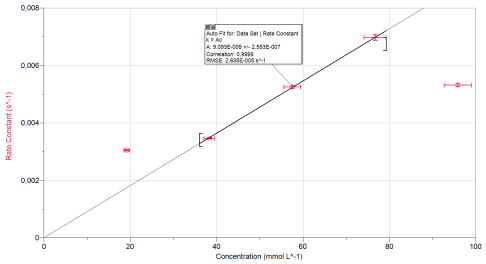

Figure 7: Data Points Plotted

This fit gives the specific rate constant $k_{\text{spec}} \approx 0.00009093\ s^{-1}\ \text{mM}^{-1} = 0.0054558\ \text{min}^{-1}\ \text{mM}^{-1}$, which is within an acceptable range of the known $k_{\text{pyro}} = 0.061\ \text{min}^{-1}\ \text{mM}^{-1}$ from **Section 2.2**.

4.3 Conclusion

The data support a direct, near-proportional increase of the apparent first-order rate constant k_{app} with suspended MnO_2 concentration. This matches the general expectation that more active surface yields faster reaction, but the measured specific rate is lower than literature ($0.061\ \text{min}^{-1}\,\text{mM}^{-1}$); plausible causes include incomplete O_2 capture (leakage, connector losses), variable effective surface area (agglomeration or settling of powder), the initial connection artifact, and instrument limits (pressure sensor accuracy, uncertain V_g). These uncertainties (notably $V_l \pm 3.3\%$ and sensor ± 2 kPa) moderately affect k_{app} and explain observed scatter and the anomalously low 0.05 g point, so quantitative agreement with literature is tentative though the trend is robust.

Methodological limitations with meaningful impact: reliance on headspace pressure rather than direct concentration assays, imperfect seals, limited replicates per mass and a narrow mass range, and possible temperature/stirring inconsistencies. Strengths include a clear theoretical derivation linking $P(t)$ to $[H_2O_2]$ and continuous high-frequency data collection.

Realistic, relevant improvements: use pressure-rated fittings or water-displacement

gas collection; immobilize catalyst or better disperse powder; increase replicate number and mass range; directly assay [H_2O_2] (titration or spectrophotometry) for cross-validation; calibrate sensor and measure V_g precisely. With these changes the proportional relationship can be tested more reliably and quantitative agreement improved.

References

[1] Hitham. M. Abuissa and Mohamed. M. Eleribi. "Thermodynamic and Kinetic Investigations for the Decomposition of Aqueous Hydrogen Peroxide on MnO2 and PbO Surfaces at Different Temperatures". In: *The Scientific Journal of University of Benghazi* 35.1 (June 2022). ISSN: 2790-1629. DOI: 10.37376/sjuob.v35i1.3262. URL: http://dx.doi.org/10.37376/sjuob.v35i1.3262.

[2] Si-Hyun Do et al. "Hydrogen peroxide decomposition on manganese oxide (pyrolusite): Kinetics, intermediates, and mechanism". In: *Chemosphere* 75.1 (Mar. 2009), pp. 8–12. ISSN: 0045-6535. DOI: 10.1016/j.chemosphere.2008.11.075. URL: http://dx.doi.org/10.1016/j.chemosphere.2008.11.075.

[3] Ching-Ping Huang and Yu-Hsiang Huang. "Comparison of catalytic decomposition of hydrogen peroxide and catalytic degradation of phenol by immobilized iron oxides". In: *Applied Catalysis A: General* 346 (2008), pp. 140–148. DOI: 10.1016/j.apcata.2008.05.017. URL: https://doi.org/10.1016/j.apcata.2008.05.017.

[4] Min June Kim et al. "Porous MnO2/CNT catalysts with a large specific surface area for the decomposition of hydrogen peroxide". In: *Korean Journal of Chemical Engineering* 34.8 (June 2017), pp. 2147–2153. ISSN: 1975-7220. DOI: 10.1007/s11814-017-0120-3. URL: http://dx.doi.org/10.1007/s11814-017-0120-3.

[5] C. M. Miller and R. L. Valentine. "Hydrogen peroxide decomposition and quinoline degradation in the presence of aquifer material". In: *Water Research* 29.10 (1995), pp. 2353–2359. DOI: 10.1016/0043-1354(95)00059-T. URL: https://doi.org/10.1016/0043-1354(95)00059-T.

[6] C. M. Miller and R. L. Valentine. "Mechanistic studies of surface catalyzed H_2O_2 decomposition and contaminant degradation in the presence of sand". In: *Water Research* 33.12 (1999), pp. 2805–2816. DOI: 10.1016/S0043-1354(98)00500-4. URL: https://doi.org/10.1016/S0043-1354(98)00500-4.

[7] R. L. Valentine and H. C. A. Wang. "Iron oxide surface catalyzed oxidation of quinoline by hydrogen peroxide". In: *Journal of Environmental Engineering* 124.1 (1998), pp. 31–38. DOI: 10.1061/(ASCE)0733-9372(1998)124:1(31). URL: https://doi.org/10.1061/(ASCE)0733-9372(1998)124:1(31).